Appendix A: Supplementary Stitching Results

Here we present the stitching results for the remaining image pairs used in our paper, and also demonstrate a stitching result for a full panorama using Moving DLT. As mentioned in Sec. 4 in the paper, to objectively compare the learnt warp of the different methods, *we avoid using postprocessing or de-ghosting techniques so that any misalignments remain obvious*. An exception is Photosynth's panorama tool where we can only obtain the final (most likely postprocessed) results.

Fig. 7 shows the stitching results obtained on the *chess/girl* dataset (the input images from this dataset are shown in Fig. 15). As can be seen in Fig. 7, the baseline warp (global homography via DLT on inliers) could not align the images since the views do not differ purely by rotation. Our As-Projective-As-Possible (APAP) stitching method manages to align the images with little visible artefacts. Our results are similar to those of the output obtained from Photosynth (most likely with postprocessing). For Smoothly Varying Affine warps (SVA), Dual-Homography warps (DHW) and Content-Preserving warps (CPW) significant ghosting remains. On this image pairs Autostitch was not able to produce a good result, as observed also in [9] — we therefore omit the result from Autostitch here.

Fig. 8 depicts the stitching results on the *carpark* image pair (the input images from this image pair are shown in Fig. 13). From Fig. 8, for the baseline method (global homography) and DHW serious misalignments can be observed in the images. SVA introduced some distortion in the extrapolation regions — observe the ground between the building and the grass patch — possibly due to their affine regularisation (as explained in Sec. 1.1). Autostitch introduced errors around the grass patch and side-walk areas. Photosynth produces an unexpected bending effect in the grass patch; this is most probably the side effect of the post-processing techniques. Here, CPW and our APAP present some minor errors.

Failure cases. Our method, like most image stitching methods, relies on feature detection and matching. When the number of matched feature points is low, none of the methods compared here will be able to generate satisfactory stitching results. This is clearly observable in Fig. 9 which shows the stitching results on the *rooftops* image pair (the input images from the *rooftops* are shown in Fig. 16). In this image pair the number of matched feature points is very small in certain regions (Fig. 11 shows the matches between these images; observe how the number of matches around the squared rooftops is low). The best stitching result in Fig. 9 is by Photosynth which most likely makes use of post-processing and de-ghosting techniques.

Appendix B: Panoramas

Here we demonstrate the usage of our technique to create panoramas, i.e., stitching multiple images together. Fig.10 shows the panorama results created from the *forest* dataset (the input images from the *forest* dataset can be seen in Fig. 14). As explained in Sec. 4.1, in order to build the panorama we first choose a central image to initialise the panorama and then incrementally warp the remaining images.

In this dataset there are significant exposure differences between the views. We remove exposure differences in the panorama using the relatively simple technique of feathering [17] (basically a weighted average of pixel values). The results after feathering blending for our APAP panorama can also be seen in Fig.10. For comparison purposes, we also show results from Photosynth which presents some minor errors as well.

Appendix C: Data Used in the Experiments

Most of the images used in our experiments were taken from different datasets used in other recent stitching papers. In this section we show the input (unwarped) images and the corresponding reference that makes use of them. Figs. 12, 13 and 14 show the images from the *temple*, *carpark* and *forest* pairs. These images are used by Gao et al. in [4].

Figs. 15 and 16 show the images from the *chess/girl* and *rooftops* pairs used by Lin et al. in [9].

Finally, our own *railtracks* image pair is shown in Fig. 17.

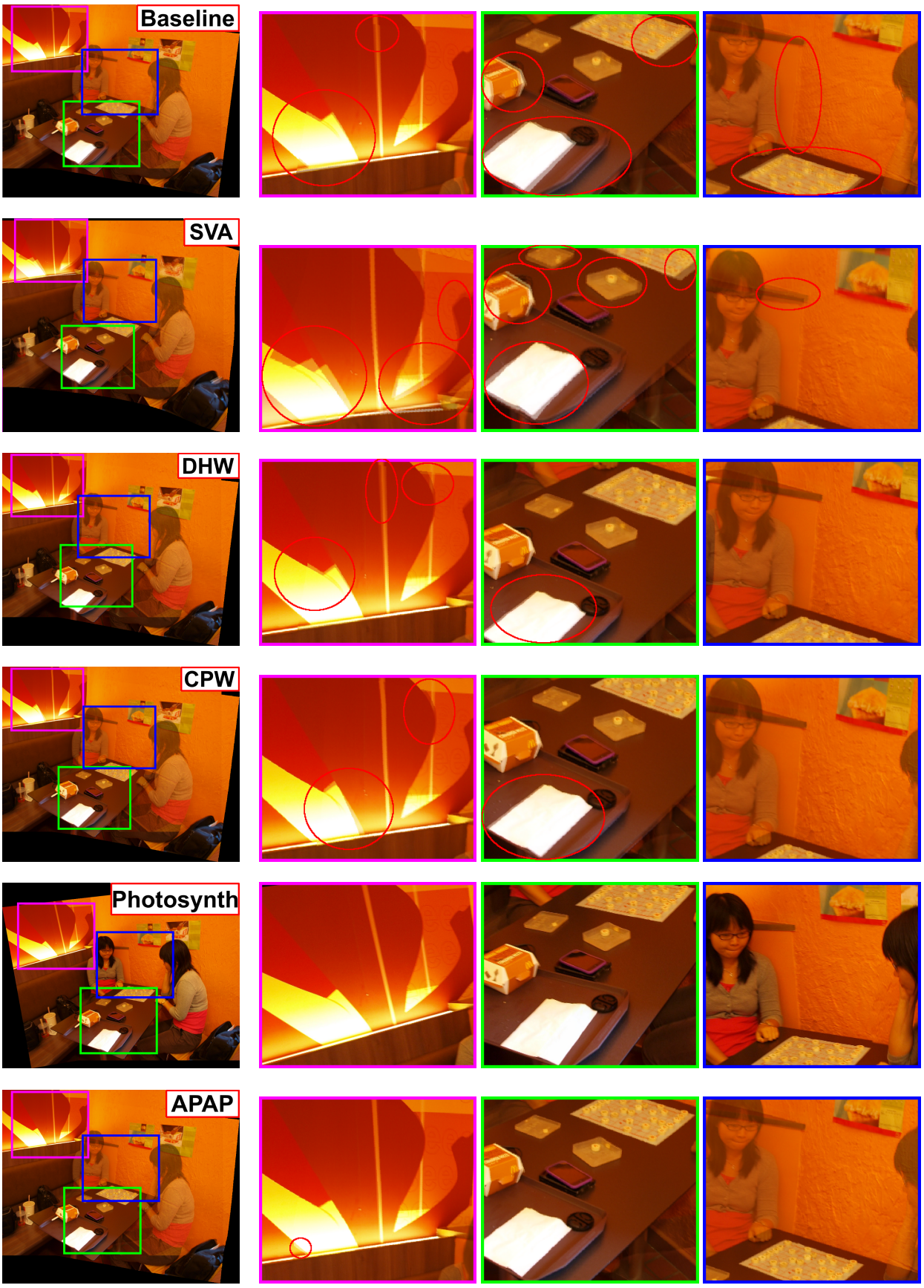

Figure 7: Qualitative comparisons (best viewed on screen) on the *chess/girl* image pair. Red circles highlight errors. List of acronyms and initialisms: SVA-Smoothly Varying Affine, DHW-Dual Homography Warps, CPW-Content Preserving Warps, APAP-As Projective As Possible Warps.

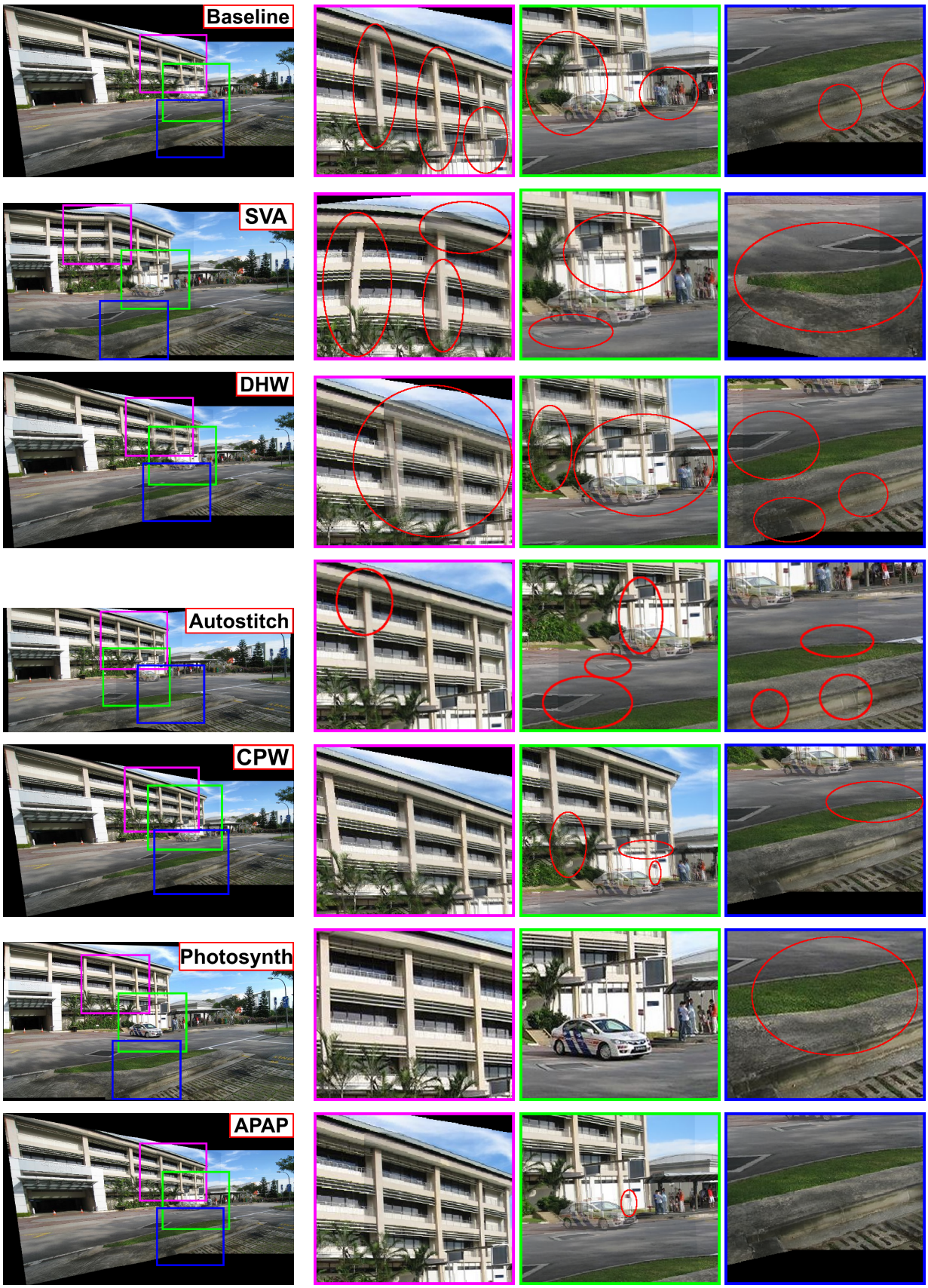

Figure 8: Qualitative comparisons (best viewed on screen) on the *carpark* image pair. Red circles highlight errors. List of acronyms and initialisms: SVA-Smoothly Varying Affine, DHW-Dual Homography Warps, CPW-Content Preserving Warps, APAP-As Projective As Possible Warps.

Figure 9: Qualitative comparisons (best viewed on screen) on the *rooftops* image pair. Red circles highlight errors. List of acronyms and initialisms: SVA-Smoothly Varying Affine, DHW-Dual Homography Warps, Auto-Autostitch, CPW-Content Preserving Warps, Photo-Photosynth, APAP-As Projective As Possible Warps.

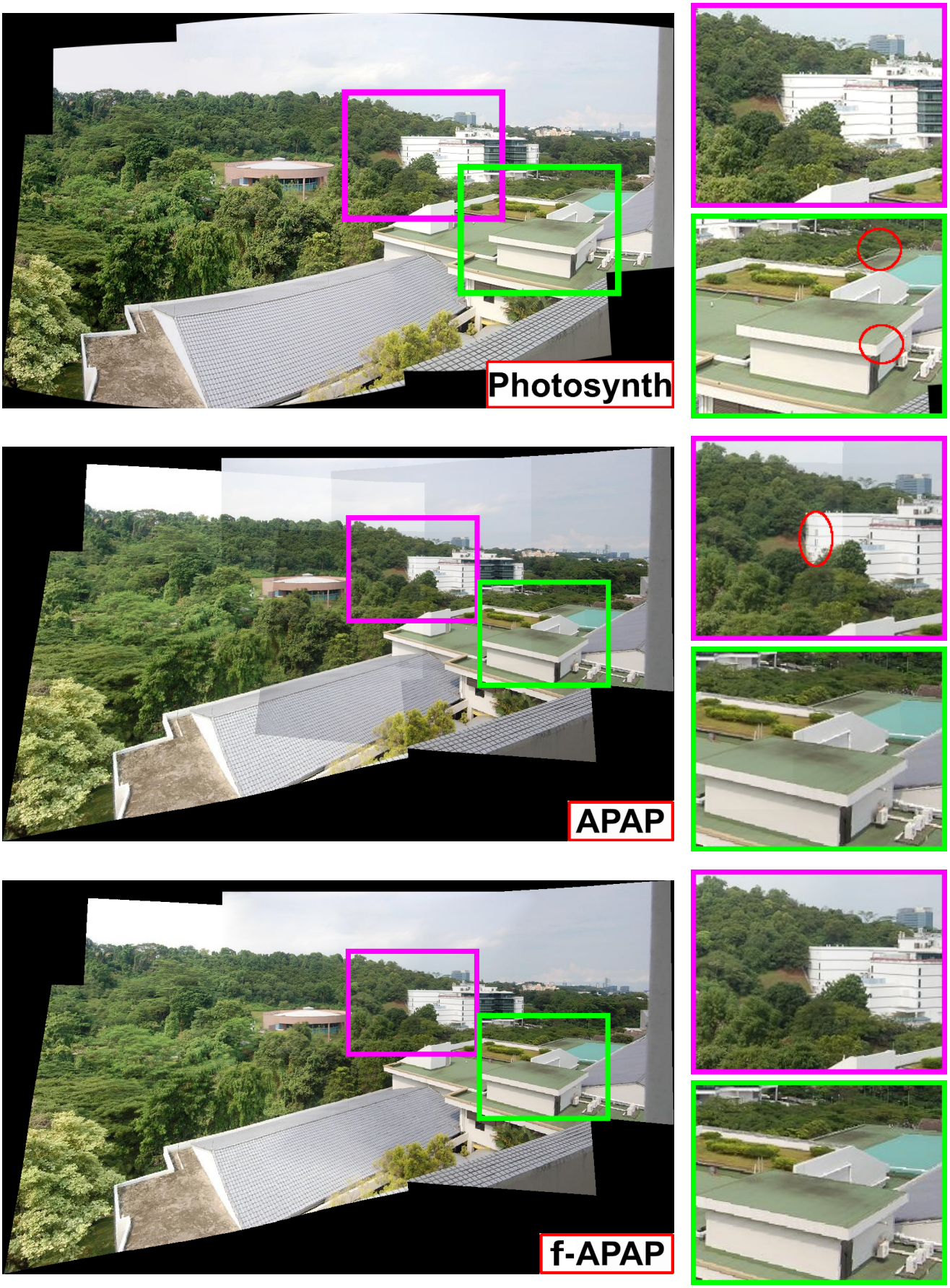

Figure 10: Panorama creation comparisons (best viewed on screen) on the *forest* dataset. Red circles highlight errors. List of acronyms and initialisms: APAP-As Projective As Possible Warps, f-APAP–As Projective As Possible warps with feathering blending.

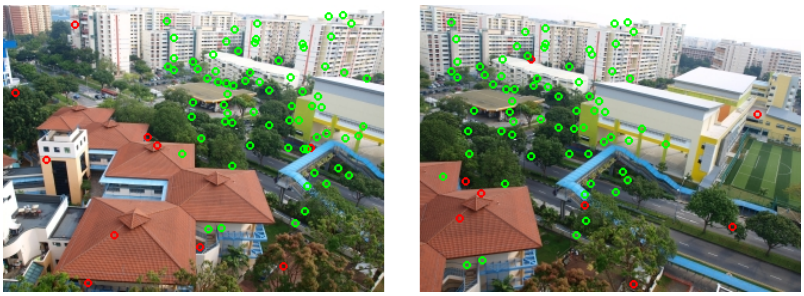

Figure 11: Feature points extracted from the *rooftops* image pair. Inliers are shown in green, outliers in red. For clarity purposes we omit the matching lines. Observe how the number of detected features around the squared rooftops is small.

Figure 12: Image pair from the *temple* dataset from [4].

Figure 13: Image pair from the *carpark* dataset from [4].

Figure 14: Images from the *forest* dataset from [4].

Figure 15: Image pair from the *chess/girl* dataset from [9].

Figure 16: Image pair from the *rooftops* dataset from [9].

Figure 17: Our *railtracks* image pair.